Defect and Diffusion Forum Vols. 297-301 (2010) pp 1340-1345
Online available since 2010/Apr/13 at www.scientific.net

doi:10.4028/www.scientific.net/DDF.297-301.1340

Diffusion in SC Ni-base Superalloy under Viscoplastic Deformation

L.A. Kommel[1, a], B.B. Straumal[2,b]

[1]Tallinn University of Technology, Ehitajate tee 5, 19086 Tallinn, Estonia

[2]Institute of Solid State Physics, Chernogolovka, Moscow District, 142432 Russia

[a]lembit.kommel@ttu.ee, [b]straumal@issp.ac.ru

Keywords: Deformation-enhanced diffusion, Ni-base superalloy, cyclic viscoplastic deformation.

Abstract. Deformation-enhanced diffusion in single-crystalline Ni-based superalloy specimens have been investigated under the conditions of hard cyclic viscoplastic tension-compression deformation. The chemical composition of phases before and after cyclic deformation was investigated by filed-emission scanning electron microscopy. At low strain amplitude values (0-0.05%; 0-0.2%; 0-0.5%) the material shows upscaled viscoelastic behavior and microstructural stability. At the increase of strain amplitude in the γ+γ'-phase (0-1%), the Ni, Re and Co content decreases, whereas Al and Mo content increases significantly. On the contrary, in the single γ'-phase area, the Ni and Co content was increased, which was accompanied by a decrease of Nb, Cr, Ta and Al content. The length of dendrite arms was significantly decreased as compared to primary dendrite arms and γ+γ'-rafts were formed parallel to the stress axis direction. As a result of the deformation-enhanced, diffusion the necking of dendrites accompanied with longitudinal cracking by the dendrite axis and cross-sectional radial cracking by interdendritic region of single crystalline specimen occurs.

Introduction

Nickel-based single crystalline (SC) possess a noticeable combination of high temperature strength, creep resistance, toughness as well as resistance to oxidation and corrosion during exploitation life [1-4]. Other metallic materials are unable to match this combination of properties at high temperatures. Depending on directional solidification parameters there are three different types of cast microstructures: equiaxed, columnar and single-crystalline. These high temperature materials can be applied for the production of turbine blades and vanes castings for turbo-jets and stationary power plants. The Ni-based superalloys used for hottest sections of turbines are subjected during exploitation to the complex fatigue loadings at high temperatures in the gas surrounding [5]. Therefore, testing in the conditions when all these effects simultaneously occur is considerably complicated. The refractory superalloys are mainly tested under tensile loading for creep resistance at high temperatures during very long time [6-9]. As a result of such tests, the "raft" γ/γ'-microstructure can be formed. The microstructure rafting takes place as a result of γ' particles coalescence by a directional coarsening via diffusion of alloying elements. The fatigue cracking at low-cycle fatigue [10] and high-cycle fatigue [11] was facilitated when the γ/γ'-rafts were perpendicular to the stress axis [12]. It was obstructed, when the γ/γ'-rafts lay parallel to stress axis [13]. Different components of SC have also different diffusion mobility [14]. At the not compensated counter-diffusion of the alloying components, the pores can be formed in the region between dendrite arms or in the interdendritic regions of SC. For example, aluminum atoms diffuse from the interdendritic region into the centre of the dendrite axis. Tungsten and rhenium atoms diffuse in the opposite direction, namely from the axis to the interdendritic regions. As a result, the dendrite arms are enriched by W, Re, Mo, and Cr while the areas between arms are enriched by Al, Ti, Nb and Ta. The mechanical properties (microhardness, Young's modulus, etc.) of the matrix γ-phase and of the γ'-phase precipitates (measured by nano-indentation and atomic force microscopy tests) depend on those composition [15] and indentation depth [16]. For example, the hardness is higher (up to 45%) for the γ'-phase precipitate regions (10.2 to 6 GPa) compared to the γ-matrix

(8.5 to 6 GPa) by the indentation depth in the interval of 0-100 nm. The reduced Young's modulus in the interval of 30-50 nm is up to 180 GPa for γ'-precipitates while matrix γ-phase shows only 150 GPa. The transversely isotropic viscoplasticity model is formulated for fatigue and creep response studies in various isothermal histories of a directionally solidified (DS) Ni-base superalloy [17]. The elasto-viscoplastic behavior of a SC Ni-base superalloy under hard cyclic viscoplastic (HCV) deformation condition is studied at room temperature in [18]. The SC superalloy shows the fully elastic behavior up to a strain of 0.6 % and instability at an increased strain [19]. Unfortunately, up to now, the influence of HCV deformation on diffusion in SC has almost not been studied. The aim of this investigation is to present the experimental results of microstructural investigations before and after HCV deformation on the diffusion and constituent phases as well as the influence of diffusion processes on mechanical properties and fracture of the SC superalloy.

Experimental

The material used in this study was the new generation SC Ni-based superalloy [3]. The alloy contains (in at. %): Al, 12.1; Cr, 5.3; Co, 9.38; Nb, 0.85; Ta, 0.89; Mo, 0.69; W, 2.4; Re, 0.88 and Ni balance [14]. This superalloy contains simultaneously Nb and Ta, but does not have any Ti. The castings have been produced by means of electro-induction melting method in a directional solidification furnace under a high vacuum. They were solidified in the [001] direction with a speed of 2-3 mm/min. For the present study the bars of SC with a diameter of 14 mm and length of ~190 mm with starter block at the conical end were manufactured. These rods were heat treated in vacuum at 1280 °C for 80 min and used for cutting off by turning the tensile test specimens (Fig. 1, a). The tensile specimens with the grip sections have an overall length of 90 mm. The gauge part has the length of 12 mm with diameter of 8 mm and a fillets radius of 6 mm. The mechanical tests of the SC Ni-based superalloy were performed at room temperature under the strain amplitude controlled regime using the Instron-8516 testing machine. For the true strain measurements, the extensometer with the base length of 10 mm was used. Cyclic loading was applied at the tension-compression with steps of strain amplitude of 0-0.05%; 0-0.2%; 0-0.5% and 0-1% at each strain values for 30 cycles, correspondingly. The tension-compression loadings were conducted under a low frequency of 0.5 Hz as constant. Samples for microstructural investigation were cut off from the gauge, transition and grip sections of the some tensile specimens (Fig. 1, a). For the microstructure evolutions via diffusion during cyclic straining study the cuts, which were cut off from different parts of samples before and after straining, were mechanically polished and etched at different times. For dissolving out of γ'-precipitates the 33 ml HNO_3 + 66 ml HCl mixture was applied. The dendrite microstructure of samples was analyzed by using the light optical microscope Nikon Microphot - FX. The chemical composition, microstructure and fracture surfaces of samples were analyzed by the high resolution field emission scanning electron microscopy (FE SEM) Zeiss ULTRA-55 and by SEM Zeiss EVOA15.

Results and Discussion

The summary strain-stress plot for true strain amplitudes of: 0-0.05; 0-0.2; 0-0.5 and 0-1% (with plastic part Set-1) is shown in Fig. 1, b. By the increase of strain amplitude, the stress amplitude values of 75, 300 and 760 MPa were increased proportionately. Material shows fully elastic behavior for 30 cycles. We suppose that during the cycling the microstructure of SC does not change significantly. The plastic deformation first appears when the tensile strain of ~0.65% at first cycle followed HCV deformation. These curves are approximately identical to a ratchetting or soft cyclic viscoelastic (SCV) deformation behavior, but only without elongation of gauge length of the sample. At the first tension cycle of HCV deformation with strain amplitude of 0-1% for the fourth test series the SC specimen at a strain of 0.65 % starts to increase in length without significantly load increase.

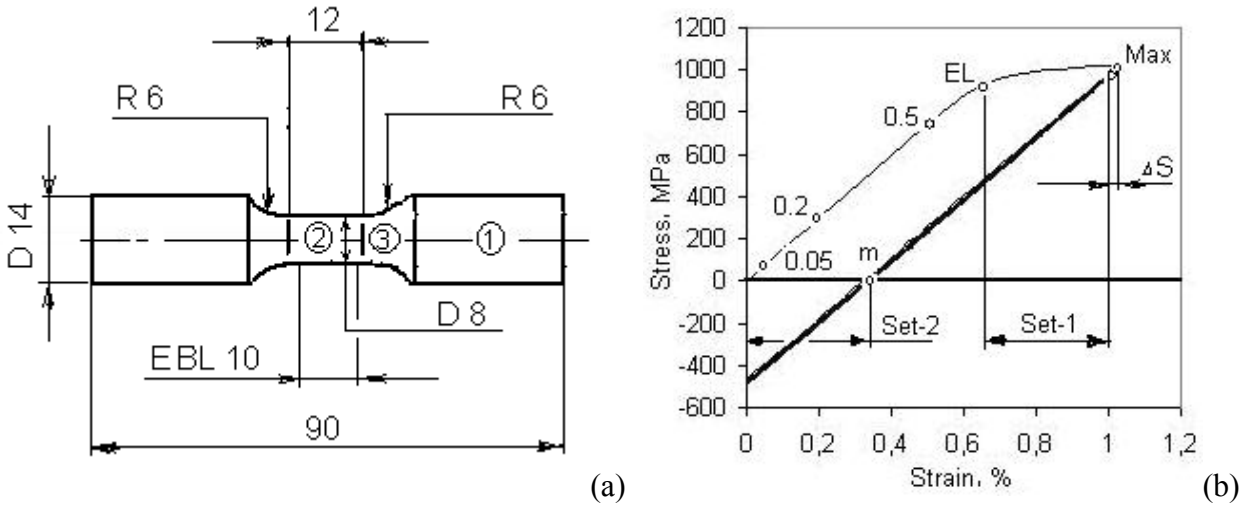

Figure 1. (a) Scheme of the test sample. (b) Summary graph for the fourth test series of the strain-stress behavior of the SC Ni-based superalloy under HCV deformation. The densifications are as follows in (a): 1, 2, and 3 – test points for microstructure and chemical condition study; EBL 10 – extensometer base length of 10 mm and in (b): EL – elastic limit (0.65%); stress-strain curves at the strain amplitudes of 0-0.05, 0-0.2 and 0-0.5%; tension curve (0-Max) at the strain amplitude of 1% at first cycle for fourth test series; ΔS = ~0.03 of strain decrease for next 29 cycles (as system error); Set-1 = Set-2 – plastic part of tensile deformation at first cycle; m – segment point, which divide the tension stress to compression stress in sample.

This strain value is pointed as EL – elastic limit point (see Fig. 1, b). At first cycle the sample was elongated up to the point "Max" which is higher 0.3% about than the strain presented. The values of strain and load accordingly were up to ΔS~3% higher than the maximum in comparison with the values for the following 29 cycles at strain of 1 %. The compression part of the first cycle and the next 29 cycles at this stage of the cyclic straining covers each other by tandem. At the increase up to 1.5 % of strain amplitude the test sample was fractured at the first cycle while the sample with no HCV deformation shows elongation up to 1.7%. The EDS investigations of microstructural features in longitudinal and in cross-section of HCV deformed gage part (designated as "After" in Tables 1 and 2, see Fig. 1, a, point 2) and no HCV deformed grip sections (designated as "Before", see Fig. 1, a, point 1) of sample. The data on the diffusion-driven concentration change for main chemical elements is presented in Table 1 and Table 2. The two areas of SC were chosen for measurements: γ+γ'-phase and single γ'-phase area. The test results are presented (in at. %) in Table 1 (γ+γ'-phase) and Table 2 (single γ'-phase). Test results show that the γ+γ'-phase or dendrite arm during HCV deformation lost via diffusion about 0.82 % of Ni, 2.48 % of Co and 7.97 % of Re. The Re content increases in γ-matrix increasing it hardness and elasticity modulus [15].

Table 1. Concentration of various elements in the γ+γ'-phase

Element	Before [at. %]	After [at. %]	Decrease [%]	Increase [%]
Ni	64.37	63.84	- 0.82	-
Al	13.58	14.35	-	+ 5.67
W	2.45	2.47	-	+ 0.81
Co	10.91	10.64	- 2.48	-
Mo	1.07	1.16	-	+ 8.41
Re	1.38	1.27	- 7.97	-
Cr	6.24	6.27	-	+ 0.48

Table 2. Concentration of various elements in the single γ'-phase

Element	Before [at. %]	After [at. %]	Decrease [%]	Increase [%]
Ni	65.81	67.55	-	+ 2.64
Al	19.86	19.20	- 3.32	-
Cr	2.93	2.49	- 15.02	-
Co	6.45	6.97	-	+ 8.06
Nb	2.34	1.53	- 34.62	-
Ta	2.62	2.26	- 13.74	-

The concentrations of Ni and Co in single γ'-phase increased in the same time (on 2.64 % and 8.06 % respectively). On the other hand, the single γ'-phase does not contain Re. The diffusion flux of various elements depends on their diffusion coefficients and liquation [14]. The detailed analysys was conducted in two key phases only. However, the investigated SC superalloy contains at least five different phases with very different concentration of elements as well. The mean compositions of these phases are presented in Table 3.

Table 3. Chemical composition (in at.%) of phases presented in the SC superalloy [23].

Phase	Ni	Al	W	Cr	Co	Mo	Re	Nb	Ta
N1	64	13	3	6.5	10.7	1	1.7	-	-
N2	62.8	16	4.3	6.9	8.9	1.1	-	-	-
N3	66.9	19	0.4	3	7	-	-	2.1	2
N4	32.9	6.7	6.2	9.3	7.6	-	-	26.9	10.4
N5	-	-	-	-	-	-	-	44	56

In Table 3 the phases are designated as: N1 - diffusive γ+γ'-phase in dendrite arm region ("After"); N2 - γ-phase after γ'-phase cuboids etching off; N3 – γ precipitations in γ'-phase eutectics; N4 – NbTa- rich region which surrounds the single γ'-phase; N5 – NbTa composition in arrows. These arrows from NbTa-compound in interdendritic regions were formed during solidification (Fig. 2, a). In Fig. 2, b the magnification from Fig. 2, a, and in Fig. 2, c the EDS spectrum from this compound are shown. Fig, 2, a shows, that the dendrite axis does not contain Nb and Ta simultaneously. According to EDS investigation, the dendrite axis after HCV deformation has only Nb but not Ta. The as-cast and HCV-fatigued samples have different mechanisms of crack forming and fracture surfaces at tension straining. In the optical micrograph of transition region (Fig. 1, a, point 3) on test sample can be seen (Fig. 3, a), that during HCV deformation the dendrite arms length in direction of (001)

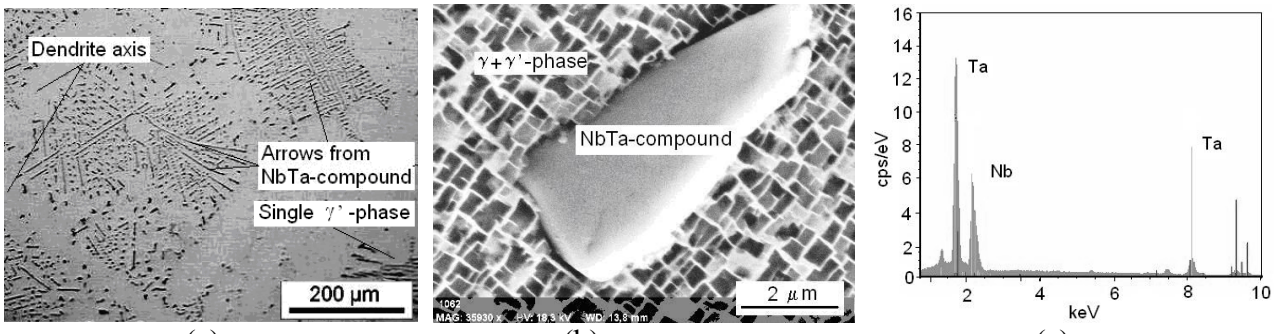

(a) (b) (c)

Figure 2. (a) Microstructure of the NbTa-compound "arrows". (b) Magnification photo of a single NbTa-arrow. (c) EDS spectrum. Designations in (a): Dendrite axis, arrows from NbTa-compound, single γ'-phase area, which is surrounded with the NbTa-rich region.

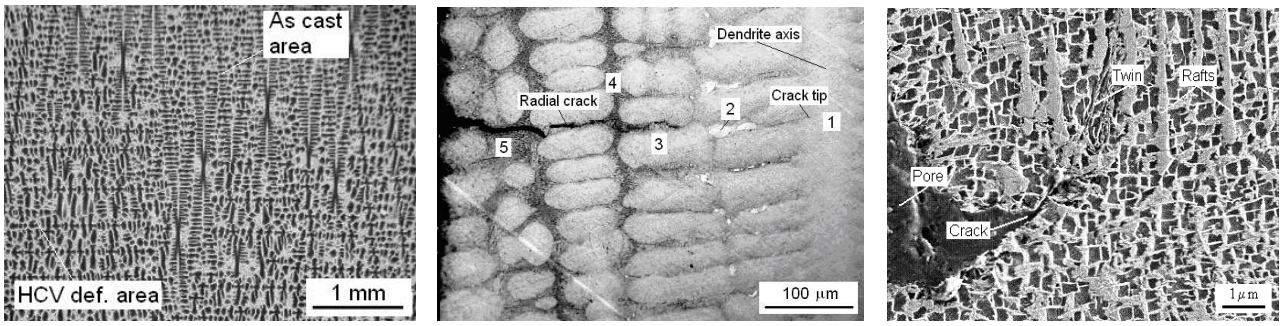

(a) (b) (c)

Figure 3. Optical micrographs of (a) SC superalloy in the transition region (see Fig. 1, a, point 3) and (b) HCV deformed area (see Fig. 1, a, point 2) radial crack with chemical composition testing points indicated. (c) SEM micrograph of crack tip in the HCV deformed part of sample. The parallel rafts, twins, cracks and pores formed before fracture can be seen.

significantly decreased (up to three times). According to these data, the NbTa-arrows were deformed identically and partly dissolved in the surrounding phase. Since the phases of SC Ni-based superalloy have different mechanical properties, which change depending on their chemical composition [19] their fracture mechanisms has to be different. As is presented by the preliminarily FE SEM investigation, the diffusion of various elements takes place during HCV deformation. The fracture mechanisms of samples are different (Fig. 3, b, c and Fig. 4. b, c). For example, in Fig. 3, a and b the radial crack is shown. In optical micrograph it can be seen that crack prolonged via the interdendritic region. The concentration of various elements near formed crack was measured in presented test points (Table 4). The crack tip is shown in Fig. 3, c with increased magnification. The prolongation of crack takes place via region where the twins were formed before. During HCV deformation the parallel to loading direction rafts were formed. Their forming will increase the fatigue life of SC. As result of opposing diffusion, the pores in this region were formed.

Table 4. Chemical compositions of phases near crack (see in Fig. 3, b)

Point	Al	Cr	Co	Ni	Nb	Mo	Ta	W	Re
1	8.03	14.47	11.80	59.37	0.25	0.50	0.43	3.14	2.00
2	12.29	12.63	7.15	62.96	1.57	0.31	1.66	1.22	0.21
3	7.60	17.08	11.43	58.46	0.20	0.34	0.55	2.66	1.68
4	7.70	19.06	11.01	56.78	0.53	0.65	0.91	1.75	1.61
5	10.30	14.47	10.95	58.87	0.63	0.46	1.03	2.32	0.96

In our study during HCV deformation of SC the Ni, Co and Re concentration was decreased in the γ+γ′-phase or in the centre of dendrite arm (Table 1). In the same time, the concentration of Al, Mo, W and Cr was increased due to the diffusion in the opposite direction. As is shown in Fig. 2, the Nb and Ta can form the “arrows” in the region between dendrite arms and near the single γ′-phase areas. The large amount of tests shows that the “arrows” contain only Ta and Nb, while the single γ′-phase areas are surrounded with the NbTa-rich interlayer. Such diffusion processes would influence different mechanical properties of the γ′-phase (like hardness, elastic modulus, toughness, plasticity etc.). The investigation of fracture surfaces shows that the fracture mechanisms are different in the cross-sectional and longitudinal directions to loading direction. The fragile fracture goes by the dendrite axis (Fig. 4, a and b) in the longitudinal direction of the HCV deformed sample. But the magnified micrograph of the surface (Fig. 4, c) of γ+γ′-phase fracture clearly demonstrates that the ductile fracture goes via cuboids of the γ′-phase and γ-phase channels with different composition.

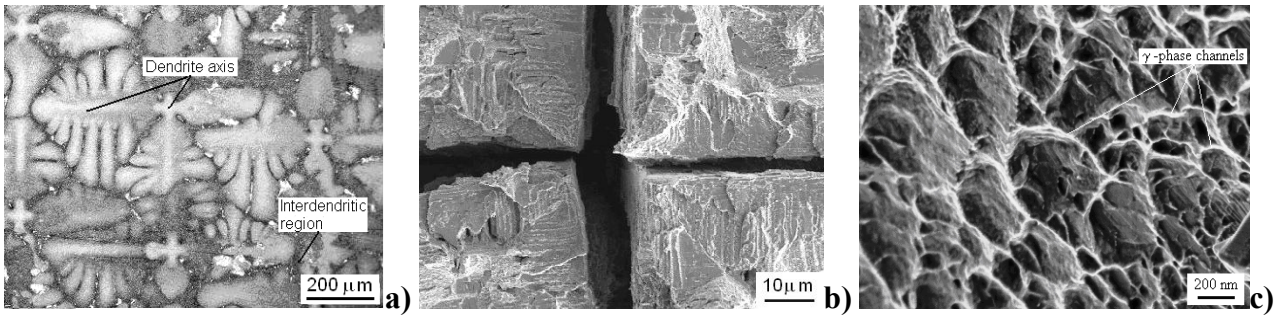

Figure 4. (a) Dendrite arms in the cross-section. (b) Fracture by the dendrite arm axis in the longitudinal direction with necking of dendrites under HCV deformation. (c) Fracture surface of samples pre-fatigued by HCV deformation, round γ+γ' – phase channels can be seen.

Conclusions

Detailed FE SEM, OM, and SEM studies of SC Ni-based superalloy before and after HCV deformation revealed that a wide variety of diffusion processes can occur depending on deformation condition and microstructure. In this brief review, the occurrence of diffusion at room temperature has been shown, and the hypothesis that the HCV deformation controlling processes is due to reordering within the strengthening factor of NbTa-compound has been discussed.

Acknowledgements

The authors would like to acknowledge support from the Estonian Foundation Grant No SF-062, Russian foundation for basic research (grant 09-03-92481) and Drs O. Volobueva and M. Viljus for SEM investigations.

References

[1] http://www.materialstechnology.org (posted in February 2007).
[2] R.C. Reed: *The Superalloys Fundamentals and Applications* (Cambridge Univ. Press, UK 2006.
[3] I.M. Razumovskii, A.V. Ruban, V.I. Razumovskiy, A.V. Logunov, V.N. Larionov, O.G. Ospennikova, V.A. Poklad and B. Johansson: Mater. Sci. Eng. A Vol. 497 (2008), p. 18.
[4] L. Kovarik, R.R. Unocic, J. Li and M.J. Mills: JOM Vol. 61 No. 2 (2009), p. 42.
[5] J.X.Zhang, H.Harada, Y.Ro, Y.Koizumi and T.Kobayashi: Acta Mater. Vol. 56 (2008), p. 2975.
[6] S. Li, J. Tao, T. Sugui and H. Zhuangqi: Mater. Sci. Eng. A Vol. 454-455 (2007), p. 461.
[7] T. Murakumo, T. Kobayashi, Y. Koizumi and H. Harada: Acta Mater. Vol. 52 (2004), p. 3737.
[8] J. Cormier, X. Milhet and J. Mendez: Mater. Sci. Eng. A Vol. 483-484 (2008), p. 594.
[9] R.C. Reed, D.C. Cox and C.M.F. Rae: Mater. Sci. Eng. A Vol. 448 (2007), p. 88.
[10] H. Zhou, Y. Ro, H. Harada, Y. Aoki and M. Arai: Mater. Sci. Eng. A Vol. 381 (2004), p. 20.
[11] Y. Liu, J.J. Yu, Y. Xu, X.F. Sun, H.R. Guan and Z.Q. Hu: Mater. Sci. Eng. A Vol. 454 (2007), p. 357.
[12] M. Ott and H. Mughrabi: Mater. Sci. Eng. A Vol. 272 (1999), p. 24.
[13] L. Shui, S. Tian, T. Jin and Z. Hu: Mater. Sci. Eng. A 418 (2006), p. 229.
[14] R. Orlov: Deformation & Fracture of Materials Vol. 6 (2008), p. 43.
[15] K. Durst and M. Göken: Mater. Sci. Eng. A Vol. 387-389 (2004), p. 312.
[16] T. Schöberl, H.S. Gupta, P. Fratzl: Mater. Sci. Eng. A Vol. 363 (2003), p. 211.
[17] M.M. Shenoy, D.L. McDowell and R.W. Neu: Int. Journal Plasticity Vol. 22 (2006), p. 2301.
[18] L. Kommel: Materials Science (Medžiagotyra) Vol. 15, No2. (2009), (In press).
[19] K. Tanaka, T. Ichitsubo, K. Kishida, H. Inui and E. Matsubara: Acta Mater. Vol. 56 (2008), p. 3786.

Diffusion in Solids and Liquids V
doi:10.4028/www.scientific.net/DDF.297-301

Diffusion in SC Ni-Base Superalloy under Viscoplastic Deformation
doi:10.4028/www.scientific.net/DDF.297-301.1340

References

[1] http://www.materialstechnology.org (posted in February 2007).

[2] R.C. Reed: The Superalloys Fundamentals and Applications (Cambridge Univ. Press, UK 2006.
doi:10.1017/CBO9780511541285

[3] I.M. Razumovskii, A.V. Ruban, V.I. Razumovskiy, A.V. Logunov, V.N. Larionov, O.G. Ospennikova, V.A. Poklad and B. Johansson: Mater. Sci. Eng. A Vol. 497 (2008), p. 18.
doi:10.1016/j.msea.2008.08.013

[4] L. Kovarik, R.R. Unocic, J. Li and M.J. Mills: JOM Vol. 61 No. 2 (2009), p. 42.
doi:10.1007/s11837-009-0026-6

[5] J.X.Zhang, H.Harada, Y.Ro, Y.Koizumi and T.Kobayashi: Acta Mater. Vol. 56 (2008), p. 2975.
doi:10.1016/j.actamat.2008.02.035

[6] S. Li, J. Tao, T. Sugui and H. Zhuangqi: Mater. Sci. Eng. A Vol. 454-455 (2007), p. 461.
doi:10.1016/j.msea.2006.11.136

[7] T. Murakumo, T. Kobayashi, Y. Koizumi and H. Harada: Acta Mater. Vol. 52 (2004), p. 3737.
doi:10.1016/j.actamat.2004.04.028

[8] J. Cormier, X. Milhet and J. Mendez: Mater. Sci. Eng. A Vol. 483-484 (2008), p. 594.
doi:10.1016/j.msea.2006.08.149

[9] R.C. Reed, D.C. Cox and C.M.F. Rae: Mater. Sci. Eng. A Vol. 448 (2007), p. 88.
doi:10.1016/j.msea.2006.11.101

[10] H. Zhou, Y. Ro, H. Harada, Y. Aoki and M. Arai: Mater. Sci. Eng. A Vol. 381 (2004), p. 20.
doi:10.1016/j.msea.2004.04.051

[11] Y. Liu, J.J. Yu, Y. Xu, X.F. Sun, H.R. Guan and Z.Q. Hu: Mater. Sci. Eng. A Vol. 454 (2007), p. 357.
doi:10.1016/j.msea.2006.11.045

[12] M. Ott and H. Mughrabi: Mater. Sci. Eng. A Vol. 272 (1999), p. 24.

doi:10.1016/S0921-5093(99)00453-0

[13] L. Shui, S. Tian, T. Jin and Z. Hu: Mater. Sci. Eng. A 418 (2006), p. 229.
doi:10.1016/j.msea.2005.11.028

[14] R. Orlov: Deformation & Fracture of Materials Vol. 6 (2008), p. 43.

[15] K. Durst and M. Göken: Mater. Sci. Eng. A Vol. 387-389 (2004), p. 312.
doi:10.1016/j.msea.2004.03.079

[16] T. Schöberl, H.S. Gupta, P. Fratzl: Mater. Sci. Eng. A Vol. 363 (2003), p. 211.
doi:10.1016/S0921-5093(03)00627-0

[17] M.M. Shenoy, D.L. McDowell and R.W. Neu: Int. Journal Plasticity Vol. 22 (2006), p. 2301.
doi:10.1016/j.ijplas.2006.03.003

[18] L. Kommel: Materials Science (Medžiagotyra) Vol. 15, No2. (2009), (In press).

[19] K. Tanaka, T. Ichitsubo, K. Kishida, H. Inui and E. Matsubara: Acta Mater. Vol. 56 (2008), p. 3786.
doi:10.1016/j.actamat.2008.04.014